ELSEVIER

Biophysical Chemistry 107 (2004) 289–298

Biophysical Chemistry

www.elsevier.com/locate/bpc

Effect of alcohols on aqueous lysozyme–lysozyme interactions from static light-scattering measurements

Wei Liu[a], Dusan Bratko[a], John M. Prausnitz[a,b], Harvey W. Blanch[a,*]

[a]*Chemical Engineering Department, University of California, Berkeley, CA 94720, USA*
[b]*Chemical Sciences Division, Lawrence Berkeley National Laboratory, Berkeley, CA 94720, USA*

Received 29 August 2003; accepted 22 September 2003

Abstract

Alcohols have been widely used as protein denaturants, precipitants and crystallization reagents. We have studied the effect of alcohols on aqueous hen-egg lysozyme self-interactions by measuring the osmotic second virial coefficient (B_{22}) using static light scattering. Addition of alcohols increases B_{22}, indicating stronger protein–protein repulsion or weaker attraction. For the monohydric alcohols used in this study (methanol, ethanol, 1-propanol, *n*-butanol, isobutanol and trifluoroethanol), B_{22} for lysozyme reaches a common plateau at approximately 5% (v/v) alcohol, while glycerol increases B_{22} more than monohydric alcohols. For a 0.05 M NaCl hen-egg lysozyme solution at pH 7, B_{22} increases from 2.4×10^{-4} to 4.7×10^{-4} ml mol/g^2 upon addition of monohydric alcohols and to 5.8×10^{-4} ml mol/g^2 upon addition of glycerol. We describe the alcohol effect using a simple model that supplements the DLVO theory with an additional alcohol-dependent term representing orientation-averaged hydrophobic interactions. In this model, the increased lysozyme repulsive forces in the presence of monohydric alcohols are interpreted in terms of adsorption of alcohol molecules on hydrophobic sites on the protein surface. This adsorption reduces attractive hydrophobic protein–protein interactions. A thicker lysozyme hydration layer in aqueous glycerol solution can explain the glycerol-increased lysozyme–lysozyme repulsion.

Keywords: Alcohols; Protein–protein interactions; Osmotic second virial coefficient; Hydrophobic interactions; Potential of mean force

1. Introduction

Protein precipitation and crystallization are common steps in the purification of proteins. Protein solubility depends on many factors, including thermodynamic properties of the solvent, temperature and pressure. Solvents used in protein precipitation and crystallization are often aqueous mixtures of

*Corresponding author. 201 Gilman Hall, Department of Chemical Engineering, University of California, Berkeley, CA 94720-1462, USA. Tel.: +1-510-642-1387; fax: +1-510-643-1228.

E-mail address: blanch@socrates.berkeley.edu (H.W. Blanch).

0301-4622/04/$ - see front matter © 2003 Elsevier B.V. All rights reserved.
doi:10.1016/j.bpc.2003.09.012

buffer salts with organic solvents, such as polymers, alcohols and polyols [1,2]. The effect of these additives on protein–protein interactions and phase behavior is poorly understood. The goal of this work is to increase our understanding of alcohol additives on protein–protein interactions and protein solution stability. Such understanding contributes toward developing a molecular-thermodynamic model for the prediction of protein solubility and phase behavior; such prediction is useful for optimizing processes to precipitate a target protein, or to obtain high-quality protein crystals.

Alcohols can induce protein helical structures, destabilize the tertiary structure of native proteins and cause some proteins to form amyloid fibrils at high concentration [3–7]. The mechanism of these effects remains unclear: it has been proposed that alcohols may act as protein-binding ligands or act indirectly through changes in solvent properties such as decreased polarity [8–11]. However, it is generally known that addition of alcohols has a strong effect on molecular interaction between macromolecules. For example, the micelle-formation process of a surfactant in aqueous solution can be significantly affected by the presence of alcohols [9]. In aqueous ethanol solution, as ethanol concentration rises, hen-egg white lysozyme exists successively in monomer, dimer, protofilament and amyloid fibrils states [12]. The tendency for lysozyme self-association in ethanol solution indicates that addition of alcohols alters the protein–protein interactions and the protein-solution phase behavior.

The osmotic second virial coefficient (B_{22}) provides a measure of the strength of protein interactions and contains information concerning the stability of a protein solution [13]: a positive B_{22} reflects overall repulsive forces between protein molecules, where protein solutions are stable; a negative B_{22}, on the other hand, indicates overall interprotein attraction that favors fluid–fluid phase separation or protein precipitation. The osmotic second virial coefficient has been related to protein solubility and used to determine favorable condition for protein crystallization [14–18]. George and Wilson [17] suggested that there exists a window of protein–protein osmotic second virial coefficients that favors crystallization: for protein crystallization, B_{22} should be in the region -2×10^{-4} to -8×10^{-4} ml mol/g^2. For solutions with B_{22} exceeding -2×10^{-4} ml mol/g^2, the protein–protein attraction is not sufficiently strong to form stable crystals, while for solution with B_{22} more negative than -8×10^{-4} ml mol/g^2, amorphous precipitations is likely.

In this work, we studied the effect of alcohols on the self-interaction of hen-egg lysozyme by measuring the osmotic second virial coefficient (B_{22}). We found that the addition of alcohols increases B_{22} at all solution conditions. The lysozyme–lysozyme interaction is described by a potential of mean force (PMF) model comprising a repulsive hard-sphere potential, an attractive dispersion potential, an electric double-layer-repulsion potential and an attractive square-well potential.

2. Materials and methods

2.1. Protein solution preparation

Hen-egg lysozyme was purchased from Boehringer Mannheim (Mannheim, Germany) and used without further purification. Methanol, ethanol, 1-propanol, *n*-butanol, iso-butanol, sodium chloride, NaOH, HCl were purchased from Fisher Scientific Company (Pittsburgh, PA). Glycerol was purchased from EM Science (Gibbstown, NJ). Trifluoroethanol (TFE) was purchased from Sigma Chemical Company (St. Louis, MO). Deionized water was obtained from a Barnested Nanopure II filtration system.

Protein stock solution ($\sim$20 g/l) was prepared by dissolving protein powder in an aqueous salt solution. Appropriate amounts of protein solution, salt solution and alcohol were mixed to achieve desired alcohol and protein concentrations. All solutions were adjusted to pH 7 using 0.1 M HCl and 0.1 M NaOH. The protein solution was filtered twice through a 0.2-μm pore-size Anotop inorganic syringe filter (Whatman) before light-scattering measurements. Protein concentration was determined by UV spectroscopy using extinction coefficient $\varepsilon_{280}=2.635$ l/g cm.

2.2. Static light scattering

Static light-scattering measurements determine the weight-average molecular weight (M_W) and the osmotic second viral coefficient (B_{22}) according to the relation [19]

$$\frac{Kc}{R(\theta)} = \frac{1}{M_W} + 2B_{22}c \quad (1)$$

where $R(\theta)$ is the excess Rayleigh scattering of the saline protein solution beyond that of the aqueous salt solution, K is the light-scattering optical constant and c is the protein mass concentration. The optical constant K depends on the solution scattering properties according to [19]

$$K = \frac{4\pi^2[n_s(dn/dc)]^2}{N_A\lambda^4} \quad (2)$$

where λ is the wavelength of the incident light, n is the refractive index of the protein solution, n_s is the refractive index of the solvent and N_A is Avagadro's number.

Static light-scattering measurements were performed using a mini-DAWN light-scattering instrument from Wyatt Technology. A 30-mW semiconductor diode laser ($\lambda = 690$ nm) was focused into a flow cell. The protein solution was continuously injected at a flow rate of 0.1 ml/min by a syringe pump. Light-scattering data were collected for a given alcohol and salt concentration, while varying the protein concentration from 1 to 10 g/l. The Rayleigh ratio was obtained from three detectors at 41.5°, 90° and 138.5°. A Zimm plot analysis [20] gave B_{22} and M_W. All the measurements were done at 25 °C.

2.3. Determination of refractive-index increment (dn/dc)

For lysozyme in NaCl solution, dn/dc has been reported to be 0.2 ml/g [21]. Addition of alcohols increases the solution refractive index and reduces dn/dc. A KMX-16 Laser Differential Refractometer (Sunnyvale, CA) was used to determine dn/dc of lysozyme in aqueous ethanol solutions. The difference between the refractive index of the solvent and that of the protein solution was measured and a linear extrapolation to zero concentration of $\Delta n/c$ vs. c yielded dn/dc. We measured dn/dc of lysozyme in 0.05 M NaCl solution with ethanol concentration 0, 20, 40 and 60% (v/v) at 25 °C. Fig. 1 shows results. The dn/dc for lysozyme in low ethanol concentration solution was interpolated from these data. The derivative dn/dc for lysozyme in other aqueous alcohol solutions was obtained by adjusting dn/dc to ensure that the correct monomer lysozyme molecular weight (~14.5 kDa) could be obtained from the Zimm plot. The same method has been used by Farnum and Zukoski to obtain dn/dc of aqueous glycerol solutions [15].

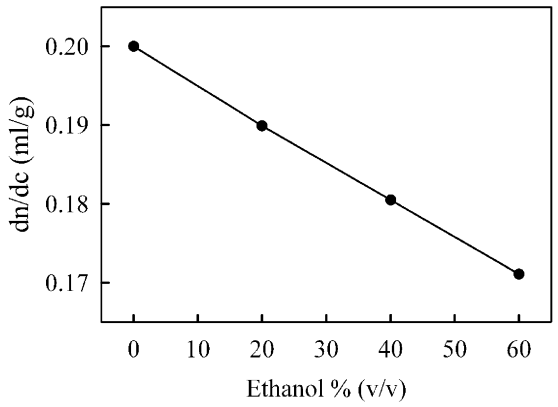

Fig. 1. Refractive-index increment, dn/dc, for aqueous hen-egg lysozyme at various ethanol concentrations in 0.05 M NaCl solution, pH 7 and 25 °C.

3. Results

3.1. The effect of ionic strength on B_{22}

The osmotic second virial coefficient (B_{22}) for aqueous hen-egg lysozyme is a strong function of solution ionic strength. Fig. 2 shows B_{22} for lysozyme in alcohol-free aqueous solutions with NaCl concentrations ranging from 0.01 to 1.0 M at pH 7. Lysozyme carries a net charge of approximately $+7e$ at pH 7 [22]. At low ionic strengths, strong electrostatic repulsion dominates protein–protein interactions and B_{22} is positive. Upon

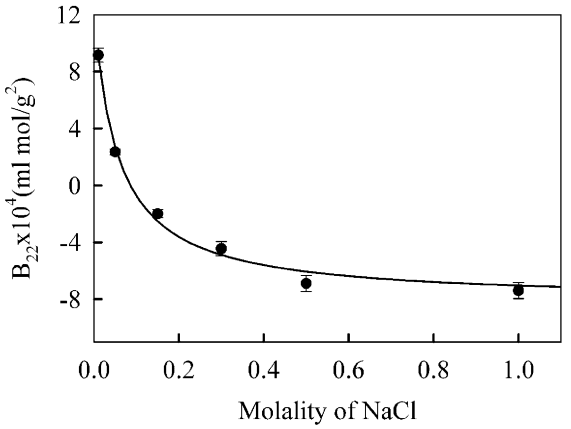

Fig. 2. Effect of ionic strength on osmotic second viral coefficient, B_{22}, for aqueous hen-egg lysozyme at pH 7 and 25 °C. The line is to guide the eye.

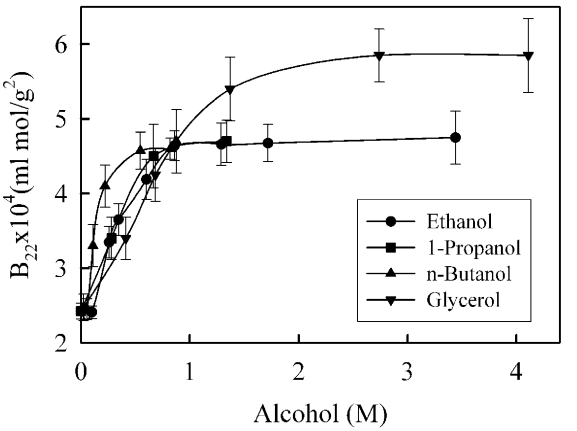

Fig. 3. Comparison of the effect of monohydric alcohols (ethanol, 1-propanol, *n*-butanol) and that of glycerol on the osmotic second virial coefficient, B_{22}, for hen-egg lysozyme in 0.05 M NaCl solution, pH 7 and 25 °C. The alcohol molar concentration is used to compare the rate of increase in B_{22} for different alcohols. The lines are to guide the eye.

Table 1
Osmotic second virial coefficients, B_{22}, for hen-egg lysozyme in aqueous 0.05 M NaCl solutions with various alcohol additives at pH 7 and 25 °C

Alcohol concentration %, (v/v)	$B_{22}\times10^{-4}$ (ml mol/g^2)	Alcohol concentration %, (v/v)	$B_{22}\times10^{-4}$ (ml mol/g^2)
0	2.4±0.2	*n*-Butanol	
		0.2	2.5±0.2
Methanol		0.5	2.5±0.2
5	4.1±0.5	1	3.3±0.3
8	4.7±0.5	2	4.1±0.3
10	4.5±0.5	5	4.6±0.2
		7	4.6±0.2
Ethanol		8	4.7±0.4
0.6	2.4±0.2		
1.5	3.4±0.2	iso-Butanol	
2	3.7±0.2	5	4.7±0.4
3.5	4.2±0.2	8	4.8±0.4
5	4.6±0.2		
7.5	4.7±0.3	TFE	
10	4.7±0.3	5	4.4±0.4
20	4.8±0.3	10	4.6±0.5
1-Propanol		Glycerol	
2	3.4±0.2	3	3.4±0.3
5	4.5±0.4	5	4.2±0.4
10	4.7±0.4	10	5.4±0.4
		20	5.8±0.4
		30	5.9±0.5

increasing ionic strength, electrostatic repulsion is screened and B_{22} becomes negative, indicating that the overall protein–protein interaction is attractive. Electrostatic forces are completely screened at ionic strengths above 0.5 M as shown in Fig. 2.

3.2. The effect of alcohols on B_{22}

We determined the osmotic second virial coefficient for aqueous hen-egg lysozyme in the presence of several alcohols (methanol, ethanol, 1-propanol, *n*-butanol, iso-butanol and TFE) and glycerol in 0.05 M NaCl solutions, at pH 7. Table 1 gives results. Addition of any alcohol raises B_{22} for lysozyme. For all the monohydric alcohols, B_{22} increases with alcohol concentration, and reaches a common plateau at approximately 5% (v/v) alcohol. Glycerol also raises B_{22} for lysozyme, consistent with Farnum and Zukoski's report that the addition of glycerol increases B_{22} for bovine pancreatic trypsin inhibitor [15]. Our data show that glycerol increases B_{22} for hen-egg lysozyme more than monohydric alcohols (Fig. 3).

Hirota et al. [23] reported that the helix-inducing ability of an alcohol is proportional to the bulkiness of its hydrocarbon groups. Alcohols with longer hydrocarbon chains such as butanol and

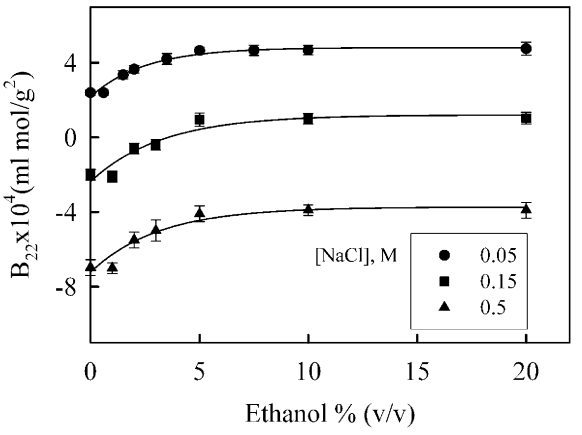

Fig. 4. The osmotic second virial coefficient, B_{22}, for hen-egg lysozyme as a function of ethanol concentration in various aqueous salt solutions, pH 7 and 25 °C. The lines are to guide the eye.

propanol are more effective in inducing protein α-helix form than shorter-chain ethanol or methanol. However, our data do not show any obvious relation between the rate of increase in B_{22} and the length of alcohol hydrocarbon chain (as shown in Fig. 3).

Fig. 4 shows B_{22} for lysozyme as a function of ethanol concentration in solutions with NaCl concentrations 0.05, 0.15 and 0.5 M at pH 7. At all solution conditions, B_{22} increases with addition of ethanol and reaches a plateau at ethanol concentrations over 5% (v/v). For a solution containing 0.15 M NaCl, B_{22} changes sign from negative to positive upon addition of ethanol, indicating that as ethanol concentration rises, protein interactions change from attractive to repulsive. The difference between B_{22} in the absence and presence of ethanol is approximately 2.5×10^{-4} ml mol/g^2, independent of NaCl concentration, suggesting that the effect of ethanol is independent of electrostatic protein–protein interactions.

At sufficiently high salt concentrations, protein aggregates form due to short-range attractions such as hydrophobic interactions. For example, Curtis et al. [24] have reported that lysozyme mutant (D101F) has a more negative osmotic second virial coefficient than native lysozyme due to increased protein–protein surface hydrophobic attractions. Lehmann et al. [25] reported that alcohols can bind to a lysozyme surface via hydrophobic interactions. Such alcohol adsorption can reduce contacts between hydrophobic patches on adjacent proteins and may explain the increased B_{22}. The apparent convergence of B_{22} values for monohydric alcohols suggests that different alcohols bind to identical sites on the protein surface and that, once adsorbed, they have a similar effect on protein–protein interaction. This effect is attributed to increased local hydrophilicity due to the solvent-exposed OH group of the adsorbed alcohol. Unlike monohydric alcohols, glycerol cannot bind to protein hydrophobic surfaces. The increase in B_{22} following addition of glycerol may be due to an increased protein hydration layer [15,26].

3.3. The effect of alcohols on protein stability

Alcohol additives affect the stability of aqueous proteins in two ways: through an effect on protein-conformation stability or on protein-solution phase stability. Protein conformational changes, including protein denaturation and partial unfolding, are the main factors leading to protein aggregation associated with some neurological diseases [27,28]. Most of the monohydric alcohols (methanol, ethanol, propanol, butanol and TFE) are protein-conformation destabilizers: they can increase protein secondary structure, disrupt protein native structure, and induce amyloid formation at high alcohol concentration [3–7]. Protein molecules also tend to assemble to form higher-order aggregates due to intermolecular attractions that are unrelated to any structural changes, which lead to protein-solution instability. Our B_{22} data show that alcohols can increase protein intermolecular repulsion at low alcohol concentration, suggesting that alcohols tend to enhance protein-solution stability. The overall effect of monohydric alcohols is to decrease protein-conformation stability and to increase protein-solution phase stability. At high alcohol concentrations, the denaturing or destabilizing effect dominates, while the solution-stabilizing effect dominates at low alcohol concentrations.

Unlike monohydric alcohols, glycerol, which is more hydrophilic, does not bind to hydrophobic patches on the protein [29]. Because glycerol

forms a nearly ideal solution with water, it fits well into the water structure. As a result, glycerol avoids the proximity of non-polar regions of the protein surface, resulting in a larger hydration layer. The glycerol concentration in the protein's hydration layer is depleted relative to that in the bulk solution [29]. This effect is known as preferential hydration of protein or preferential exclusion of co-solvent. Glycerol is a protein stabilizer and can increase both protein-conformation stability and protein-solution phase stability. In the presence of glycerol, the increased excluded volume of the protein, including the hydration layer, gives a more positive B_{22} and stronger protein–protein repulsions [15,26,29]. At the same time, the folded protein, which has a smaller surface area, exhibits lower preferential exclusion than that observed for denatured states where the solvent exposed-area is larger. This preferential exclusion effect stabilizes the protein's native conformation in aqueous glycerol solutions.

4. The potential of mean force

Interactions between two protein molecules in solution can be quantified through a PMF. The negative derivative of PMF with respect to distance is the force between two protein molecules at infinite dilution. In mixed solvents, the PMF requires configuration averaging for all mixed-solvent components [30]; in the present case, the mixed-solvent includes water, alcohol and salt ions. If the PMF, W_{22}, is isotropic, the osmotic second virial coefficient, B_{22}, is related to W_{22} by [31]

$$B_{22} = -\frac{1}{2}\frac{N_A}{M_W^2}\int_0^\infty 4\pi r^2\left[\exp\left(-W_{22}(r)/kT\right)-1\right]\mathrm{d}r \tag{3}$$

where r is the center-to-center separation of the two solute molecules, N_A is Avogadro's number, T is the absolute temperature and k is Boltzmann's constant.

For globular proteins, the PMF can be approximated by

$$W_{22}(r) = W_{hs}(r) + W_{elec}(r) + W_{disp}(r) + W_{spec}(r) \tag{4}$$

where, $W_{hs}(r)$ is the protein hard-sphere (excluded-volume) potential; $W_{elec}(r)$ is the electric double-layer-repulsion potential; $W_{disp}(r)$ is the attractive dispersion potential, and $W_{spec}(r)$ is a square-well potential, to account for protein–protein specific interactions including hydrophobic attractions, hydrogen bonds and salt bridges [32]. The first three terms, $W_{hs}(r)$, $W_{elec}(r)$ and $W_{disp}(r)$ are described by DLVO theory [33].

The hard-sphere potential is [33]

$$W_{hs} = \begin{cases} \infty \text{ for } r \leqslant \sigma \\ \\ 0 \text{ for } r > \sigma \end{cases} \tag{5}$$

where $\sigma = d + 2s$, is the effective spherical diameter of a protein; d is the protein hard-sphere diameter from crystal-structure data, and s is the thickness of the protein's hydration layer. Hen-egg lysozyme ($45\times30\times30$ Å) [34], can be approximated as a globular molecule with a hard-sphere diameter $\sim$34.4 Å. From dynamic light scattering measurements [35], the lysozyme hydration layer, s, was estimated to be 1 Å and assumed independent of ionic strength and pH.

The potential due to electric double-layer repulsion is derived from Debye–Hückel theory [33]:

$$W_{elec}(r) = \frac{z^2e^2\exp[-\kappa(r-d)]}{4\pi r\varepsilon_o\varepsilon_r(1+\kappa d/2)^2} \quad \text{for } r > \sigma \tag{6}$$

where ze is the effective charge of the protein, e is the elementary charge, ε_o is the dielectric permittivity of vacuum, ε_r is the dielectric constant of water and κ is the inverse of the Debye length, given by

$$\kappa^2 = \frac{2e^2N_AI}{kT\varepsilon_o\varepsilon_r} \tag{7}$$

where I is the ionic strength of the solution.

The attractive (Hamaker) dispersion potential is [36]

$$W_{\mathrm{disp}}(r) = -\frac{H}{12}\left\{\frac{d^2}{r^2-d^2} + \frac{d^2}{r^2} + 2\ln\left(1-\frac{d^2}{r^2}\right)\right\} \quad \text{for } r \geqslant \sigma \tag{8}$$

where H is the effective Hamaker constant for protein–protein interaction, considered independent of salt concentration [37,38]. For proteins in aqueous solution, $H = 5kT$ provides a reasonable approximation [37].

The strength of inter-protein interaction can vary with local surface composition, leading to repulsion for hydrophilic and attraction for hydrophobic patches. Such orientation-dependent hydrophobic attractions along with other short-range interactions including hydrogen bonds and salt bridges can be approximated by a site-specific attractive potential [39]:

$$\phi(x) = \begin{cases} -\varepsilon_{\mathrm{spec}} & \text{for } x \leqslant \delta \\ 0 & \text{for } \delta < x \end{cases} \tag{9}$$

where x is the site–site distance, $\varepsilon_{\mathrm{spec}}$ is the square-well depth and δ is the width of the square well. The spherically symmetric square-well potential, $W_{\mathrm{spec}}(r)$, is calculated from the orientation-averaged $\phi(x)$. Because the osmotic second virial coefficient accounts for interactions between two lysozyme molecules, $\delta = 0.134\sigma$ was chosen to ensure no association beyond monomer–dimer association [39]. In the present work, $\varepsilon_{\mathrm{spec}}$, is a fitting parameter obtained from experimental second virial coefficient data.

5. Potential of mean force calculation

There are two adjustable parameters in our PMF model: the protein effective charge ze and the square-well depth $\varepsilon_{\mathrm{spec}}$. The effective charge on the protein may differ from that for a crystal or as obtained from titration data [22]. The difference is attributed to ion binding by the protein [40,41]. In addition, because DLVO theory neglects attractive charge-dipole and dipole–dipole attractions

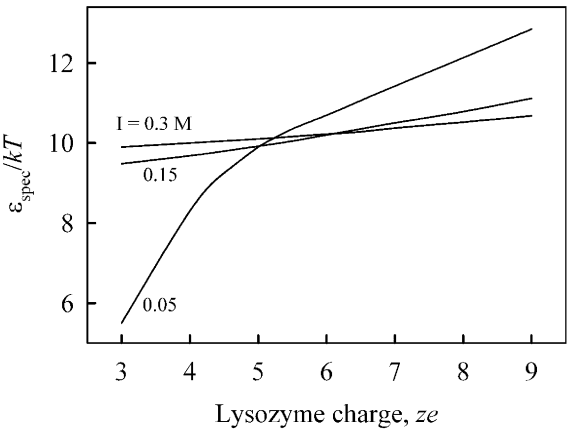

Fig. 5. Determining effective lysozyme charge, ze and square-well depth, $\varepsilon_{\mathrm{spec}}$, from experimental data.

[42,43], further reduction of the protein effective charge may be needed to bring model calculations close to experiment. At pH 7, hen-egg lysozyme carries a charge $+9e$ according to its crystal structure [44], and approximately $+7e$ based on hydrogen-ion titration [39]. However, when applied to data similar to ours, the appropriate protein charge lies between $+5$ and $6e$, independent of solution ionic strength [45–47]. For several low ionic strengths, a curve was generated representing the set of ($\varepsilon_{\mathrm{spec}}$, ze) points that bring the calculated B_{22} into agreement with experiment. The intersection of these curves for different ionic strengths corresponds to desired values of $\varepsilon_{\mathrm{spec}}$ and ze. Fig. 5 shows this method to determine $\varepsilon_{\mathrm{spec}}$ and ze from our experimental data. We obtained $\varepsilon_{\mathrm{spec}} = 9.9kT$ and $ze = +5.1e$.

For aqueous alcohol solutions, dielectric constant, ε_{r}, decreases linearly with alcohol molarity [23]. The decreased ε_{r} enhances protein–protein electrostatic repulsion. The experimental B_{22} reaches a plateau (Fig. 4) as ethanol concentration increases to $\sim$5% (v/v). However, addition of 5% ethanol changes ε_{r} only slightly, from 78.5 to $\sim$76 [23]. When the ionic strength is 0.5 M or above, the electrostatic repulsion is completely screened as shown in Fig. 2. Nevertheless, addition of ethanol increases B_{22} from -7×10^{-4} to -4.5×10^{-4} ml mol/g^2 (Fig. 4) in 0.5 M NaCl solution. Therefore, ethanol does not affect the

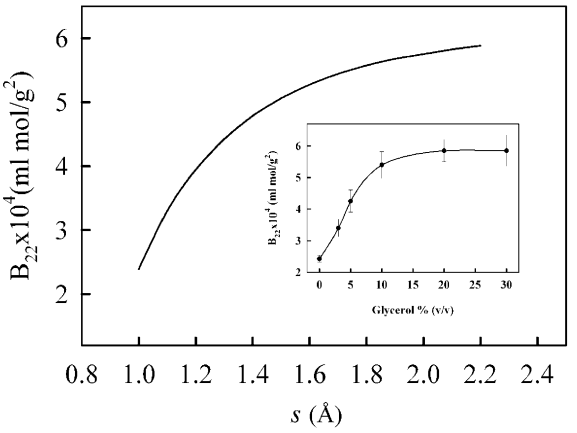

Fig. 6. The effect of protein hydration layer thickness, *s*, on the second virial coefficient, B_{22}, predicted from the PMF model in 0.05 M NaCl solution, pH 7. Inset: B_{22} as a function of glycerol concentration at the same solution conditions.

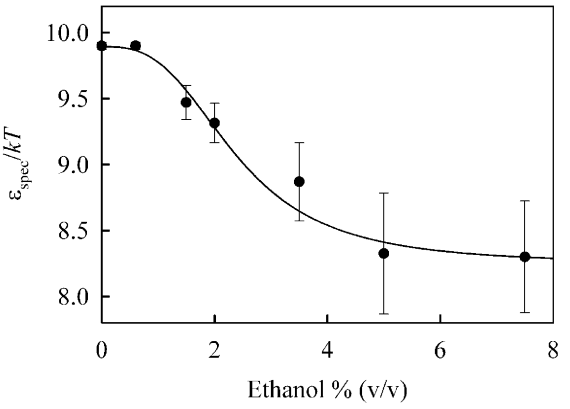

Fig. 7. Square-well depth, ε_{spec}, as a function of ethanol concentration in 0.05 M NaCl solution, pH 7. The line is to guide the eye.

protein–protein interaction through electrostatic interactions. The same conclusion is also reported by Farnum and Zukoski [15].

Chirico et al. [26] reported that in 60% (w/w) glycerol solution, the hydrodynamic radius of hen-egg lysozyme is approximately 1.6 Å larger than that in glycerol-free solution. The increased hydrodynamic radius in presence of glycerol is caused mainly by the increased protein hydration layer [15,29], which will affect the closest approach for two protein molecules in solution. Fig. 6 shows the osmotic second virial coefficient, B_{22}, as a function of protein hydration layer, *s*, predicted from our PMF model. The increase in hydration layer by approximately 1 Å can change B_{22} sufficiently to account for the effect of glycerol as shown in Fig. 6. Unlike glycerol, monohydric alcohols are unable to increase the protein hydration layer or hydrodynamic radius. Instead, ethanol slightly decreases lysozyme's hydrodynamic radius [48], which may result in a decrease of B_{22} due to reduced excluded volume. But our results show B_{22} increasing with addition of ethanol. We do not consider any change of protein effective radius in our subsequent calculations.

Fig. 7 shows square-well depth, ε_{spec}, as a function of ethanol concentration in 0.05 M NaCl solution. The square-well depth, ε_{spec}, approximately 9.9*kT* in the absence of ethanol, decreases to 8.4*kT* upon addition of 5% (v/v) of ethanol. The reduced square-well depth, approximately 1.5*kT*, corresponds to a bond energy near 3.7 kJ/mol at 25 °C, a reasonable value for protein–protein hydrophobic interactions that are reduced by addition of ethanol.

6. Conclusions

We have measured the osmotic second virial coefficient of hen-egg lysozyme in salt solution with several alcohol additives. All the alcohols used in this study raise the second virial coefficient, indicating stronger protein–protein repulsion. Protein solution stability is thereby enhanced. We have described the monohydric alcohol effect on protein–protein interaction through an attractive square-well potential. The reasonable square-well depth data obtained support the view that alcohols are protein-binding ligands. When glycerol is used as an additive, experimental result indicates that glycerol provides a thicker hydration layer leading to stronger protein–protein hard-sphere repulsion. The results reported here may be useful in selection of optimal conditions for protein processing.

Acknowledgments

This work was supported by the National Science Foundation under Grant No. BES-0118208,

and by the Office of Basic Energy Sciences of the US Department of Energy.

References

[1] A. Mcpherson, Crystallization of macromolecules: general principles, Method Enzymol. 114 (1985) 113–125.
[2] K. Cai, J.L.C. Miller, C.J. Stenland, et al., Solvent-dependent precipitation of prion protein, Biochim. Biophys. Acta 1597 (2002) 28–35.
[3] S. Goda, K. Takano, Y. Yamagata, et al., Amyloid protofilament formation of hen egg lysozyme in highly concentrated ethanol solution, Protein Sci. 9 (2000) 369–375.
[4] M.R.H. Krebs, D.K. Wilkins, E.W. Chung, et al., Formation and seeding of amyloid fibrils from wild-type hen lysozyme and a peptide fragment from the β-domain, J. Mol. Biol. 300 (2000) 541–549.
[5] K. Shiraki, K. Nishikawa, Y. Goto, Trifluoroethanol-induced stabilization of the α-helical structure of β-lactoglobulin: implication for non-hierarchical protein folding, J. Mol. Biol. 245 (1995) 180–194.
[6] A. Kurono, K. Hamaguchi, Structure of muramidase (lysozyme), VII. Effect of alcohols and the related compounds on the stability of muramidase, J. Biochem. 56 (1964) 432–440.
[7] K. Ikeda, K. Hamaguchi, Interaction of alcohols with lysozyme, J. Biochem. 68 (1970) 785–794.
[8] D. Eagland, in: F. Franks (Ed.), Water: a comprehensive treatise, vol. 4, Plenum Press, New York, 1975, pp. 305–518.
[9] G. Onori, S. Passeri, A. Cipiciani, Role of hydrophobic interactions on the melting of transfer-RNA molecules and on the micellization process, J. Phys. Chem. 93 (1989) 4306–4310.
[10] C. Tanford, Protein denaturation. Part A. Characterization of the denatured state, Adv. Protein Chem. 23 (1968) 121–217.
[11] P.D. Thomas, K.A. Dill, Local and nonlocal interactions in globular proteins and mechanisms of alcohol denaturation, Protein Sci. 2 (1993) 2050–2065.
[12] Y. Yonezawa, S. Tanaka, T. Kubota, K. Wakabayashi, K. Yutani, S. Fujiwara, An insight into the pathway of the amyloid fibril formation of hen egg white lysozyme obtained from a small-angle X-ray and neutron scattering study, J. Mol. Biol. 323 (2002) 237–251.
[13] A. George, Y. Chiang, B. Guo, A. Arabshahi, Z. Cai, W.W. Wilson, Second viral coefficient as predictor in protein crystal growth, Meth. Enzymol. 276 (1997) 100–110.
[14] B. Guo, S. Kao, H. McDonald, A. Asanov, L.L. Combs, W.W. Wilson, Correlation of second viral coefficients and solubilities useful in protein crystal growth, J. Cryst. Growth 196 (1999) 424–433.
[15] M. Farnum, C. Zukoski, Effect of glycerol on the interactions and solubility of bovine pancreatic trypsin inhibitor, Biophys. J. 76 (1999) 2716–2726.
[16] B.L. Neal, D. Asthagiri, A.M. Lenhoff, Molecular origins of osmotic second viral coefficients of proteins, Biophys. J. 75 (1998) 2469–2477.
[17] A. George, W.W. Wilson, Predicting protein crystallization from a dilute solution property, Acta Crystallogr. D 51 (1994) 361–365.
[18] D.F. Rosenbaum, C.F. Zukoski, Protein interactions and crystallization, J. Cryst. Growth 169 (1996) 752–758.
[19] W.H. Stockmayer, Light scattering in multi-component systems, J. Chem. Phys. 18 (1950) 58–61.
[20] B.H. Zimm, The scattering of light and the radial distribution function of high polymer solutions, J. Chem. Phys. 16 (1948) 1093–1099.
[21] W.J. Fredericks, M.C. Hammonds, S.B. Howard, F. Rosenberger, Density, thermal expansivity, viscosity and refractive index of lysozyme solutions at crystal growth concentrations, J. Cryst. Growth 141 (1994) 183–192.
[22] R.A. Curtis, J.M. Prausnitz, H.W. Blanch, Protein–protein and protein–salt interactions in aqueous protein solutions containing concentrated electrolytes, Biotechnol. Bioeng. 57 (1998) 11–21.
[23] N. Hirota, K. Mizuno, Y. Goto, Group additive contributions to the alcohol-induced α-helix formation of melittin: implication for the mechanism of the alcohol effects on proteins, J. Mol. Biol. 275 (1998) 365–378.
[24] R.A. Curtis, C. Steinbrecher, M. Heinemann, H.W. Blanch, J.M. Prausnitz, Hydrophobic forces between protein molecules in aqueous solutions of concentrated electrolyte, Biophys. Chem. 98 (2002) 249–265.
[25] M.S. Lehmann, S.A. Mason, G.J. McIntyre, Study of ethanol–lysozyme interactions using neutron diffraction, Biochemistry 24 (1985) 5862–5869.
[26] G. Chirico, S. Beretta, G. Baldini, Conformation of interacting lysozyme by polarized and depolarized light scattering, J. Chem. Phys. 110 (1999) 2297–2304.
[27] G. Forloni, N. Angeretti, R. Chiesa, et al., Neurotoxicity of a prion protein-fragment, Nature 362 (1993) 543–546.
[28] D.M. Walsh, A. Lomakin, G.B. Benedek, M.M. Condron, D.B. Teplow, Amyloid β-protein fibrillogenesis: detection of a protofibrillar intermediate, J. Biol. Chem. 272 (1997) 22364–22372.
[29] S.N. Timasheff, T. Arakawa, Mechanisms of protein precipitation and stabilization by co-solvents, J. Cryst. Growth 90 (1988) 39–46.
[30] W.G. McMillan, J.E. Mayer, The statistical thermodynamics of multicomponent systems, J. Chem. Phys. 13 (1945) 276–350.
[31] T.L. Hill, Theory of solutions, J. Am. Chem. Soc. 79 (1957) 4885–4890.
[32] C. Branden, J. Tooze, Introduction to Protein Structure, Garland Publishing, New York, 1991.
[33] E.J.W. Verwey, J.T.K. Overbeek, Theory of the Stability of Lyophobic Colloids, Elsevier, Amsterdam, 1948.

[34] C.C.F. Blake, D.F. Koenig, G.A. Mair, A.C.T. North, D.C. Phillips, V.R. Sarma, Structure of hen egg-white lysozyme, Nature 206 (1965) 757–770.
[35] Y. Georgalies, A. Zouni, W. Eberstein, W. Saenger, Formation dynamics of protein precrystallization fractal clusters, J. Cryst. Growth 126 (1993) 245–260.
[36] H.C. Hamaker, The London-Van-der Waals attraction between spherical particles, Physica IV 10 (1937) 1058–1072.
[37] S. Nir, Van der Waals interactions between surfaces of biological interest, Prog. Surf. Sci. 8 (1976) 1–58.
[38] J. Israelachvili, Intermolecular and Surface Forces, second ed., Academic Press, San Diego, 1991.
[39] M.S. Wertheim, Fluids of dimerizing hard spheres and fluid mixtures of hard spheres and dispheres, J. Chem. Phys. 85 (1986) 2929–2936.
[40] D. Bratko, D. Henderson, Counterion binding in the solvation shell of ionic colloids in aqueous solution, Electrochim. Acta 36 (1991) 1761–1768.
[41] P. Linse, Structure, phase stability, and thermodynamics in charged colloidal solutions, J. Chem. Phys. 113 (2000) 4359–4373.
[42] D. Bratko, A. Striolo, J.Z. Wu, H.W. Blanch, J.M. Prausnitz, Orientation-averaged pair potentials between dipolar proteins or colloids, J. Phys. Chem. B 106 (2002) 2714–2720.
[43] A. Striolo, D. Bratko, J.Z. Wu, N. Elvassore, H.W. Blanch, J.M. Prausnitz, Forces between aqueous nonuniformly charged colloids from molecular simulation, J. Chem. Phys. 116 (2002) 7733–7743.
[44] M.S. Weiss, G.J. Palm, R. Hilgenfeld, Crystallization, structure solution and refinement of hen egg-white lysozyme at pH 8.0 in the presence of MPD, Acta Crystallogr. D 56 (2000) 952–958.
[45] D.E. Kuehner, C. Heyer, C. Rämsch, U.M. Fornefeld, H.W. Blanch, J.M. Prausnitz, Interactions of lysozyme in concentrated electrolyte solutions from dynamic light-scattering measurements, Biophys. J. 73 (1997) 3211–3224.
[46] W. Eberstein, Y. Georgalis, W. Saenger, Molecular interactions in crystallizing lysozyme solutions studied by photon correlation spectroscopy, J. Cryst. Growth 143 (1994) 71–78.
[47] M. Muschol, F. Rosenberger, Interactions in undersaturated and supersaturated lysozyme solutions: static and dynamic light scattering results, J. Chem. Phys. 103 (1995) 10424–10432.
[48] A. Bonincontro, A.D. Francesco, M. Matzeu, G. Onori, A. Santucci, Conformational changes of lysozyme in water–ethanol mixtures, Colloids Surf. B: Biointerfaces 10 (1997) 105–111.